PHYSICAL REVIEW B **76**, 100507(R) (2007)

Dispersive collective charge modes in an incommensurately modulated cuprate Mott insulator

L. Wray,[1] D. Qian,[1] D. Hsieh,[1] Y. Xia,[1] H. Eisaki,[2] and M. Z. Hasan[1,3]
[1]*Department of Physics, Joseph Henry Laboratories of Physics, Princeton University, Princeton, New Jersey 08544, USA*
[2]*Nanoelectronics Research Institute (NeRI), AIST, Central 2, Tsukuba, Ibaraki 305-8568, Japan*
[3]*Princeton Center for Complex Materials, Princeton University, Princeton, New Jersey 08544, USA*
(Received 30 May 2007; revised manuscript received 31 July 2007; published 19 September 2007)

We report measurement of collective charge modes of insulating $Sr_{14}Cu_{24}O_{41}$ using inelastic resonant x-ray scattering over the complete Brillouin zone. Our results show that the intense excitation modes at the charge gap edge predominantly originate from ladder-containing planar substructures. The observed modes are found to be dispersive for momentum transfers along the "legs" ($\hbar\vec{Q}\|\hat{c}$) but nearly localized along the "rungs" ($\hbar\vec{Q}\|\hat{a}$). We show that the dispersion and peak width characteristics of the modes can be understood in the strong-coupling quantum limit (Hubbard $U \gg t_{ladder} > t_{chain}$, where t is the hopping parameter). Quite generally, we demonstrate that the momentum tunability ($\vec{Q}$ resolution) of inelastic x-ray scattering can be utilized to resolve mode contributions in multicomponent incommensurate quantum electron systems.

DOI: 10.1103/PhysRevB.76.100507 PACS number(s): 74.72.Jt, 71.90.+q, 72.80.Sk, 78.70.Ck

The evolution of charge dynamics with dimensional crossover is one of the most fundamental themes in strongly correlated electron systems. For example, in one-dimensional (1D) systems electrons exhibit charge-spin separation[1] and in 2D superconductivity appears upon doping.[2] The electron behavior in materials with somewhat *intermediate dimensionality* is poorly understood but of great current interest.[3–7] The doped cuprate series $Sr_{14-x}Ca_xCu_{24}O_{41}$ exhibits unusual quantum magnetism, electron-phonon coupling, charge order, and superconductivity under high pressure (T_c up to $\sim$12 K at $P>3$ GPa), and shares many unconventional properties that are also observed in the 2D cuprates.[4–7] Unlike 1D (Sr_2CuO_3 or $SrCuO_2$) or 2D (La_2CuO_4 or Nd_2CuO_4) cuprates, the structurally incommensurate cuprate system $Sr_{14}Cu_{24}O_{41}$ (SCO) consists of two Cu-O structural units as stacked planes of chains and two-leg ladders. Photoemission spectroscopy, which gives a measure of the momentum-resolved band structure, is limited due to charging, cleavage, and surface issues in this compound.[8]

Recent developments show that momentum-resolved inelastic x-ray scattering is highly sensitive in distinguishing between propagating charge excitations in chainlike[9,10] (1D) and planar[11] (2D) networks. It is also capable of revealing the nature of the electronic correlations via the measurement of detailed momentum transfer dependence of the excitations along different crystallographic directions.[9–12] Such measurements provide the essential components for identifying an effective theory of electronic behavior of correlated insulators.[2,3,9–13] The inelastic x-ray charge spectrum of 1D cuprates[9,10] exhibits radically different behavior from that of the 2D cuprates.[11] In 1D, a strongly dispersive holon resonance[9] with half-periodic spinonlike onset is observed,[10] whereas in 2D excitonlike modes with Zhang-Rice character dominate.[11] In this Rapid Communication, we present an inelastic resonant x-ray scattering (RIXS) study of $Sr_{14}Cu_{24}O_{41}$ to elucidate the nature of the interplay between the reduced dimensionality, lattice substructures, and electronic correlations by exploring the Q space. A systematic analysis of our data suggests that the electron-hole pair modes in $Sr_{14}Cu_{24}O_{41}$, in the vicinity of the gap edge, predominantly originate from the quasi-two-dimensional ladder planes, and in some respects resemble collective charge motion observed in 1D cuprates rather than that found in the 2D systems where superconductivity is observed.

The compound $Sr_{14}Cu_{24}O_{41}$ contains two copper oxide planar sublattices, one composed of Cu_2O_3 two-leg ladders [Fig. 1(a)] and one forming edge-sharing CuO_2 chains. These lattices are incommensurate in the axial (c_L) direction, and roughly seven ladder unit cells correspond to ten chain units ($7c_L \sim 10c_{ch}$). The system is also inherently hole doped; however, it has been suggested that most holes are localized and reside on the chain planes.[6] The samples were grown using an optical floating-zone method, and the experiments were performed at ambient temperatures and pressure using the high-flux undulator beamline 9-ID at the Advanced Photon Source. Inelastic scattering was measured by varying $Q=(4\pi/\lambda)\sin\theta$ (λ is the wavelength of x rays while 2θ is the scattering angle) along the $\hat{a}$ and $\hat{c}$ axes of single-crystalline $Sr_{14}Cu_{24}O_{41}$. The chain compound $SrCuO_2$ was studied for comparison and Nd_2CuO_4 is also briefly examined as a model quasi-two-dimensional compound that (like SCO and $SrCuO_2$) lacks an apical oxygen outside the Cu-O plaquette. Incident polarization for all spectra was maintained perpendicular to the Cu-O plaquette. The scattered

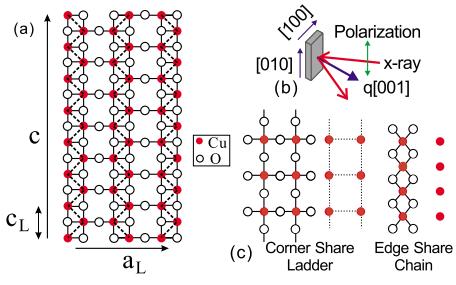

FIG. 1. (Color online) Lattice substructures and scattering geometries. (a) Ladder unit cell in $Sr_{14}Cu_{24}O_{41}$. (b) Scattering geometry configured with E field aligned in the [010] (b-axis) direction. (c) Two distinct Cu-O substructural units. The bonding between two adjacent ladders is very weak.

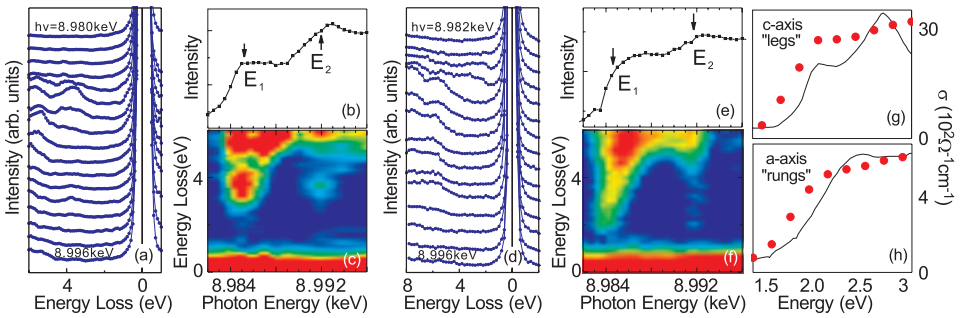

FIG. 2. (Color) Inelastic resonance profiles. (a) Energy dispersion curves for incident energy dependence of $SrCuO_2$ at momentum transfer $Q=\pi$ along the chain direction, with incident photon energy ($h\nu$) from 8.980 (top) to 8.996 keV (bottom). (b) Observed resonance energies E_1 and E_2 in the total fluorescence yield Cu K edge absorption. (c) Energy dispersion curves shown in (a) plotted in color to display more clearly the two resonance energies that couple to valence band charge excitations. (d) Energy dispersion curves for $Sr_{14}Cu_{24}O_{41}$ at $Q=2\pi/c_L$ with $h\nu$ from 8.982 to 8.996 keV, showing two resonances, labeled on the plot of fluorescence in (e). (f) Curves shown in (d) are plotted in color. Inelastic charge response for $Sr_{14}Cu_{24}O_{41}$ at 8.984 keV incident energy and $Q=2\pi$ along the (g) $\hat{c}$ and (h) $\hat{a}$ axes with polarization along the $\hat{b}$ axis, compared with optical conductivity data (solid line) with (g) $\hat{c}$- and (h) $\hat{a}$-axis polarization. (Ref. 6) The onset of DOS is in good agreement with x-ray response for $\sim 2\pi/c_L$ [ladder Brillouin Zone (BZ) center].

beam was reflected from a diced Ge(733)-based analyzer for energy analysis and focused onto a solid-state detector that was thermoelectrically cooled to achieve a low level of background noise. Under these configurations, the experimental apparatus achieved a resolution of 320 meV.

Coupling of the x-ray scattering process to specific excitations relies on resonance with intermediate charge excitations, and is dependent on the incident photon energy. Therefore, we first thoroughly investigate the detailed incident energy behavior of the excitation modes, and the summary of results is shown in Fig. 2. The spectral weight of low-energy excitations across the optical gap (charge transfer or Mott gap) is enhanced for incident x-ray energies near E_1 =8.9845 keV and E_2=8.992 keV. For low-dimensional systems, particularly in 1D, it is generally found that, if the incident x-ray energy is tuned near the absorption peak (E_1 in Fig. 1), electron-hole excitations near the insulating gap edge [similar to an optical edge, Figs. 2(g) and 2(h)] are excited through the resonance process. The broad momentum dispersion (E vs Q) of the excitations reflects the excitation modes expected in the charge dynamic response, although lineshape and cross-section effects, such as the relative spectral intensity as a function of energy loss, vary in detail.[9–12] The incident-energy-dependent inelastic profile of the ladder (Fig. 2) is qualitatively similar to that of the chain $SrCuO_2$, which has been shown to exhibit[10] a broad representation of the expected intrinsic charge response based on density matrix renormalization group calculations.[10] This was also shown to be the case in numerical exact diagonalization studies of the Hubbard model in 1D.[12]

The momentum dependence along the $\hat{c}$ direction is shown in Figs. 3(a)–3(c) as measured near the E_1 resonance of $Sr_{14}Cu_{24}O_{41}$. An upward trend in intensity in the direction of greater energy loss is seen in all curves, due to intense spectral features at $E>4.5$ eV. These higher-energy spectral features, arising out of various interband transitions, appear to be almost dispersionless, and have been subtracted when fitting the lower-energy spectral weight. A broad, flat-topped feature is seen between 2 and 4.5 eV in all curves, and can be fitted well with two 1.2 eV width Lorentzians separated by ~1 eV, as shown at the bottom of Fig. 3(a). The low-energy peaks are slightly more distinct at 8.984 keV than at 8.9845 keV; however, a feature at 5.3 eV energy loss is only clearly visible at 8.9845 keV. A dip between these features is visible in the BZ center and at the zone edge [Figs. 3(a) and

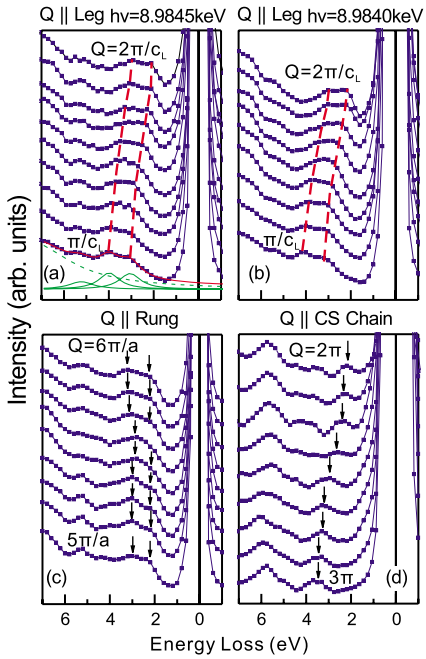

FIG. 3. (Color online) Q dependence of charge modes. Energy dispersion curves are shown for the RIXS spectrum at incident energies ($h\nu$) of (a) 8.984 and (b) 8.9845 keV, with momentum transfer in the ladder direction from $Q=2\pi/c_L$ (top) to π/c_L (bottom). The dispersion of low-energy features is traced with red dashed lines, and a fitting (described in the text) is shown for features in the bottom curve of (a). (c) Low-energy features (black arrows) have no measurable dispersion in the $\hat{a}$ direction, shown from $Q=6\pi$ (top) to 5π with incident energy 8.9845 keV. Intensity scale in (c) is smaller than in (b) by a factor of 2. (d) Low-energy excitation feature in single-chain $SrCuO_2$, measured from $Q=2\pi$ to 3π, exhibits a similar dispersion to the ladder peaks but has one peak.

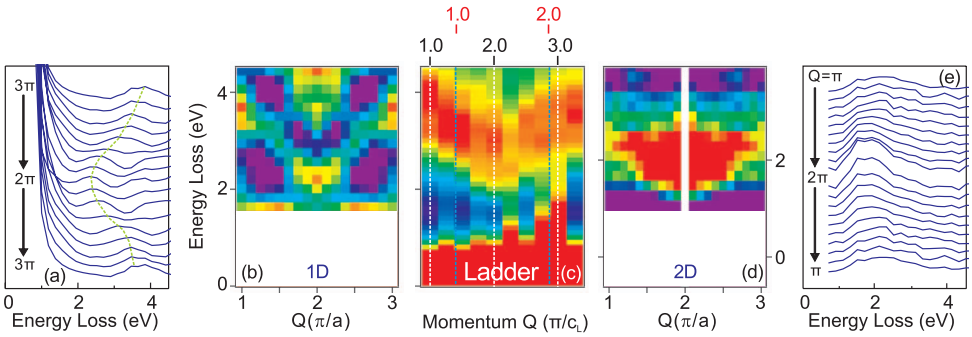

FIG. 4. (Color) Q dependence and lattice dimensionality. Inelastic charge response spectral weight across the Brillouin zone for (a),(b) quasi-1D $SrCuO_2$, (c) $Sr_{14}Cu_{24}O_{41}$, and (d),(e) quasi-2D Nd_2CuO_4. Spectra were measured from (a),(b) $Q=2\pi$ to 3π, (c) $Q=\pi$ to 3.25π, and (d), (e) π to 2π, and (a), (b) and (d), (e) show data symmetrized about $Q=2\pi$. Color images in (b) and (d) represent the curves displayed in (a) and (e), respectively. In (c), red ticks mark the positions in the chain BZ and black ticks mark positions in the ladder BZ. Low-energy (~2–4.5 eV) spectral weight is found to be periodic with the ladder.

3(b)]. Tracing the peaks [red lines in Fig. 3(a)] yields a dispersion of ~1 eV, which is larger than that typically observed in 2D prototype cuprates,[11] but similar to the dispersion of $SrCuO_2$. Figure 3(c) shows momentum transfer along the $\hat{a}$ direction (ladder "rung"). The low-energy features have no measured dispersion along this direction, but appear to come slightly closer together near $Q=\pi/2$ and $Q=\pi$.

An image plot with momentum transfer across the full second-ladder Brillouin zone is shown in Fig. 4(c). The low-energy features ($1.5<E<4.5$ eV) of SCO are roughly symmetric about $Q=2\pi/c_L$, and no signal corresponding to the chain periodicity is observed. Dispersion over the second half of the second Brillouin zone ($Q=2\pi-3\pi$) appears to be smaller than from $Q=\pi$ to 2π by less than 0.1 eV, which is of the same order as the previously estimated interladder coupling [~0.026 eV,[14] yellow lines in Fig. 1(a)], and may be due to the true $4\pi/c_L$ ladder plane periodicity. Dispersion in quasi-two-dimensional compounds, such as Nd_2CuO_4 shown in Fig. 4(d), is much smaller in the Cu-O bond direction, and is accompanied by a large damping of intensity across the Brillouin zone, with intensity weakest at the zone boundary. By contrast, the corner-sharing single-chain compound is thought to have only a single ~1.1 eV dispersion low-energy charge excitation peak, with enhanced spectral weight at the Brillouin zone edge.[10].

The experimentally measured dispersion and peak intensity of the two features observed in SCO fall between those of 1D and 2D systems, implying a continuous transition between distinct 1D and 2D charge dynamics. In order to understand the results, we consider a variation of the 1D strong-coupling limit ($U\gg t$) in which the excited electron-hole pairs of a single-band Hubbard model are unaffected by local spin.[13] In a renormalized picture, the dispersion of free "hole" and "double-occupancy" quasiparticles that are separated from the spin background is given by $2t_L\cos(kc_L)\pm t_\perp$ in the ladder and $2t_{ch}\cos(kc_{ch})$ in the chain, with t_L representing nearest-neighbor hopping in the ladder structure $\hat{c}$-axis direction and $t_\perp$ giving hopping across the ladder rungs. These bands are expected to be split by the on-site Coulomb interaction (Hubbard U). Such a band structure has been used to interpret the infrared spectrum, which probes charge excitations with $Q=0$.[14] The term "interband continuum" is adopted to refer to RIXS spectral weight associated with excitations between a specific pair of occupied and unoccupied bands, in contrast with bound particle-hole "exciton" excitation modes that are also possible within the strong-coupling model when nearest-neighbor Coulomb interaction is included. We have plotted the renormalized band structure and the allowed regions of interband transition spectral weight for such a model in Fig. 5, with the experimentally measured dispersion of low-energy RIXS features overlaid for comparison. The experimentally measured dispersion of the two lowest-energy RIXS features follows the lower edges of the top and bottom interband continua. It has been analytically shown that in a 1D strong-coupling model in the presence of intersite Coulomb interaction, most spectral weight concentrates near the lower edge of the continuum.[13]

Now we discuss the apparent absence of the chain layer band. The absence or weakness of the signal can be understood in the strong-coupling limit too. The charge-transfer energies in the ladder and chain substructures of $Sr_{14}Cu_{24}O_{41}$ are similar in magnitude [on the order of 1.5–3 eV (Refs. 6 and 14)], so the spectral intensities from the ladder and chain are expected to overlap in the energy window of interest. We mark with hatching the regime of the lower-energy signal from the chain in Fig. 5 based on Refs. 6 and 14. In the strong-coupling limit, the spectral intensity of the charge response is proportional to the square of the scaled hopping parameters ($|N(\vec{Q},\omega)|\sim t^2/U^2$).[13] The chain substructures are edge shared (Fig. 1), therefore direct hopping is very small compared to hopping along the legs of the ladder, leading to a relatively large contribution of spectral intensity due to the Cu_2O_3 ladder substructure compared to that from the CuO_2 chain-containing planes. This is further confirmed by the large magnitude (~1 eV) of the measured dispersion (Fig. 3). The weakness of the hopping integral for the edge-sharing chain suggests that the associated mode must be very weakly dispersive (essentially flat), in contrast to the observed Q dependence of experimental peaks in the relevant charge-transfer energy range. Finally, the experimentally observed periodicity of the dispersion relations corresponds to $2\pi/c_L$ but not $2\pi/c_{ch}$ [Fig. 4(c)]. Therefore, the predominant contribution is due to the ladder layer.

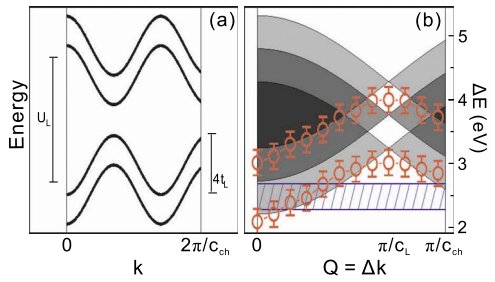

FIG. 5. (Color online) Two-particle charge spectrum. (a) Renormalized band structure of the ladder. Splitting is due to rung coupling. (b) Energy range of all possible two-particle excitations in the ladder based on (a). Regions with spectral weight from more than one band pair (continuum) are darker. Experimental peak positions determined from Fig. 3 are overlaid [red (gray) circles] for comparison. Hatched regions (2.3–2.7 eV) mark the experimental boundaries for the two-particle spectrum of the chain layer, which is expected to overlap with the ladder continuum, based on Ref. 14.

The experimentally observed charge dynamics along the rung direction can be understood in the following qualitative scheme. Since the interladder virtual electron hop is via a 90° exchange path, its magnitude is small compared to the intraladder hopping, so the pair excitation near the gap edge is mainly confined to the individual ladder units and propagates (hence is dispersive) along the leg direction of the ladder units. This is consistent with our finding of the lack of dispersion of excitation modes along the $\hat{a}$ direction [Fig. 3(c)], as well as weaker spectral intensity. This scenario, and the fact that the dispersion behavior is similar to that of the corner-sharing chain compound [Fig. 3(d)], at least near the insulating gap edge, support the quasi-one- (riverlike) dimensionality of the collective charge excitation modes in $Sr_{14}Cu_{24}O_{41}$. Such collective charge dynamics are significantly different from what is typically observed in most two-dimensional cuprates.[11] The charge dynamics in ladders also differs in details from that in 1D, in the sense that no half-periodic spinonlike onset[10] is observed. This is possibly due to suppression of charge-spin separation in the ladder geometry because of dimer coupling in the rungs.[6]

In conclusion, our results demonstrate that the low-energy excitation modes at the gap edge in $Sr_{14}Cu_{24}O_{41}$ predominantly originate from the ladder-containing layers. The measured dispersion relations of the low-energy modes and distribution of spectral weight fall between what is typically observed in analogous 1D and 2D systems, suggesting distinct physics associated with intermediate dimensionality. We suggest that the traits of such a collective mode spectrum can be described in the strong-interaction limit by lateral confinement of electron-hole pairs, although a complete description requires a multiband resonant calculation with a very large unit cell.[15]

Note added. Another recent study[16] performed along the leg direction is in agreement with our observation. Our study of the rung direction allows us to further demonstrate that inelastic resonant scattering can be utilized to resolve mode contributions in incommensurate quantum systems in general.

We gratefully acknowledge D. Huse, E. Isaacs, R. S. Markiewcz, T. Gog, and D. Casa. This work is primarily supported by DOE Grant No. DE-FG-02-05ER46200. The use of APS is supported by DOE W-31-10-Eng-38.

[1] E. L. Lieb and F. Y. Wu, Phys. Rev. Lett. **20**, 1445 (1968); C. Kim, A. Y. Matsuura, Z.-X. Shen, N. Motoyama, H. Eisaki, S. Uchida, T. Tohyama, and S. Maekawa, *ibid.* **77**, 4054 (1996).

[2] P. A. Lee, N. Nagaosa, and X.-G. Wen, Rev. Mod. Phys. **78**, 17 (2006) and references therein.

[3] M. Imada, A. Fujimori, and Y. Tokura, Rev. Mod. Phys. **70**, 1039 (1998).

[4] E. M. McCarron III *et al.*, Mater. Res. Bull. **23**, 1355 (1988).

[5] E. Dagotto and T. M. Rice, Science **271**, 618 (1996); S. Sachdev, *ibid.* **288**, 475 (2000).

[6] For a recent review on $Sr_{14}Cu_{24}O_{41}$, see A. Gozar and G. Blumberg in *Frontiers in Magnetic Materials*, edited by A. V. Narlikar (Spinger-Verlag, Berlin, 2005), pp. 653–695.

[7] T. Osafune, N. Motoyama, H. Eisaki, S. Uchida, and S. Tajima, Phys. Rev. Lett. **82**, 1313 (1999); P. Abbamonte, G. Blumberg, A. Rusydi, A. Gozar, P. G. Evans, T. Siegrist, L. Venema, H. Eisaki, E. D. Isaacs, and G. A. Sawatzky, Nature (London) **431**, 1078 (2004).

[8] T. Takahashi, T. Yokoya, A. Ashihara, O. Akaki, H. Fujisawa, A. Chainani, M. Uehara, T. Nagata, J. Akimitsu, and H. Tsunetsugu, Phys. Rev. B **56**, 7870 (1997).

[9] M. Z. Hasan, P. A. Montano, E. D. Isaacs, Z.-X. Shen, H. Eisaki, S. K. Sinha, Z. Islam, N. Motoyama, and S. Uchida, Phys. Rev. Lett. **88**, 177403 (2002).

[10] Y.-J. Kim, J. P. Hill, H. Benthien, F. H. L. Essler, E. Jeckelmann, H. S. Choi, T. W. Noh, N. Motoyama, K. M. Kojima, S. Uchida, D. Casa, and T. Gog, Phys. Rev. Lett. **92**, 137402 (2004).

[11] M. Z. Hasan, E. D. Isaacs, Z.-X. Shen, L. Miller, K. Tsutsui, T. Tohyama, and S. Maekawa, Science **288**, 1811 (2000); Y.-J. Kim, J. P. Hill, S. Komiya, Y. Ando, D. Casa, T. Gog, and C. T. Venkataraman, Phys. Rev. B **70**, 094524 (2004); E. Collart, A. Shukla, J.-P. Rueff, P. Leininger, H. Ishii, I. Jarrige, Y. Q. Cai, S.-W. Cheong, and G. Dhalenne, Phys. Rev. Lett. **96**, 157004 (2006).

[12] K. Tsutsui, T. Tohyama, and S. Maekawa, Phys. Rev. B **61**, 7180 (2000); T. P. Devereaux, G. E. D. McCormack, and J. K. Freericks, Phys. Rev. Lett. **90**, 067402 (2003); T. Nomura and J. I. Igarashi, Phys. Rev. B **71**, 035110 (2005); J. v. d. Brink, M. v. Veenendaal, Europhys. Lett. **73**, 121 (2006); R. S. Markiewicz and A. Bansil, Phys. Rev. Lett. **96**, 107005 (2006).

[13] This results from the perturbative ground-state description.

[14] Z. V. Popovic, M. J. Konstantinovic, V. A. Ivanov, O. P. Khuong, R. Gajic, A. Vietkin, and V. V. Moshchalkov, Phys. Rev. B **62**, 4963 (2000).

[15] R. S. Markiewicz (unpublished).

[16] K. Ishii, K. Tsutsui, T. Tohyama, T. Inami, J. Mizuki, Y. Murakami, Y. Endoh, S. Maekawa, K. Kudo, Y. Koike, and K. Kumagai, Phys. Rev. B **76**, 045124 (2007).